



BASIC SCIENCE ARTICLE

Short exposure to hyperoxia causes cultured lung epithelial cell mitochondrial dysregulation and alveolar simplification in mice

David Garcia¹, Jennifer F. Carr², Felix Chan², Abigail L. Peterson², Kimberlyn A. Ellis², Alejandro Scaffa³, Andrew J. Ghio⁴, Hongwei Yao² and Phyllis A. Dennerly^{2,5,6}

BACKGROUND: Prolonged exposure to high oxygen concentrations in premature infants, although lifesaving, can induce lung oxidative stress and increase the risk of developing BPD, a form of chronic lung disease. The lung alveolar epithelium is damaged by sustained hyperoxia, causing oxidative stress and alveolar simplification; however, it is unclear what duration of exposure to hyperoxia negatively impacts cellular function.

METHODS: Here we investigated the role of a very short exposure to hyperoxia (95% O₂, 5% CO₂) on mitochondrial function in cultured mouse lung epithelial cells and neonatal mice.

RESULTS: In epithelial cells, 4 h of hyperoxia reduced oxidative phosphorylation, respiratory complex I and IV activity, utilization of mitochondrial metabolites, and caused mitochondria to form elongated tubular networks. Cells allowed to recover in air for 24 h exhibited a persistent global reduction in fuel utilization. In addition, neonatal mice exposed to hyperoxia for only 12 h demonstrated alveolar simplification at postnatal day 14.

CONCLUSION: A short exposure to hyperoxia leads to changes in lung cell mitochondrial metabolism and dynamics and has a long-term impact on alveolarization. These findings may help inform our understanding and treatment of chronic lung disease.

Pediatric Research (2021) 90:58–65; <https://doi.org/10.1038/s41390-020-01224-5>

IMPACT:

- Many studies use long exposures (up to 14 days) to hyperoxia to mimic neonatal chronic lung disease.
- We show that even a very short exposure to hyperoxia leads to long-term cellular injury in type II-like epithelial cells.
- This study demonstrates that a short (4 h) period of hyperoxia has long-term residual effects on cellular metabolism.
- We show that neonatal mice exposed to hyperoxia for a short time (12 h) demonstrate later alveolar simplification.
- This work suggests that any exposure to clinical hyperoxia leads to persistent lung dysfunction.

INTRODUCTION

Many studies have shown that prolonged exposures to supra-physiologic oxygen levels (hyperoxia) lead to oxidative stress and lung alveolar injury.^{1–3} However, in newborns, even a brief exposure to hyperoxia in the delivery room can be injurious.^{4,5} Furthermore, whether there are longer-term consequences of a short exposure to hyperoxia occurs is not clear.

Type II alveolar epithelial cells (AECs) are responsible for the biosynthesis and secretion of pulmonary surfactant and are progenitors of type I AECs, which serve to facilitate oxygen diffusion into capillaries.⁶ Type II cells have high energy demands due to their continuous synthesis and release of pulmonary surfactant. Type II cells rely on mitochondria for the production of acetyl-CoA, allowing for the generation of phospholipids.⁷ Consequently, these cells contain three times the amount of

mitochondrial volume per cell than any other lung cell and the number and size of their mitochondria are reduced upon differentiating to type I AECs.^{8,9}

Mitochondria form intracellular interconnected dynamic networks, and their shape and size are altered in order to meet cellular metabolic demands.¹⁰ Fusing of mitochondrial populations occurs in response to cellular or mitochondrial stress and during normal mitochondrial turnover.¹⁰ Cells such as lung microvascular endothelial cells, which are more glycolytic and less dependent on oxidative phosphorylation (oxphos), have mitochondria with a punctate appearance.¹¹ Type II AECs exposed to cytotoxic cigarette smoke, which primarily depend on oxphos, display more fusion and the formation of elongated mitochondrial networks.¹²

The mouse lung epithelial cell line MLE-12 expresses pulmonary surfactant proteins B and C and mimics a type II AEC model. It has

¹Department of Chemistry, Brown University, Providence, RI, USA; ²Department of Molecular Biology, Cell Biology and Biochemistry, Brown University, Providence, RI, USA;

³Department of Molecular Pharmacology, Physiology, and Biotechnology, Brown University, Providence, RI, USA; ⁴US Environmental Protection Agency, Chapel Hill, NC, USA;

⁵Department of Pediatrics, Warren Alpert Medical School, Brown University, Providence, RI, USA and ⁶Hasbro Children's Hospital, Providence, RI, USA

Correspondence: Phyllis A. Dennerly (phyllis_dennerly@brown.edu)

These authors contributed equally: David Garcia, Jennifer F. Carr

Received: 19 June 2020 Revised: 7 October 2020 Accepted: 13 October 2020

Published online: 3 November 2020

been shown that MLE cell lines recapitulate type II AEC metabolic phenotypes, specifically with respect to oxygen exposure.¹³ Previously it was shown that a 24-h exposure of these cells to hyperoxia reduced overall oxphos as well as the activities of respiratory complexes I and II.¹⁴ However, it is not known whether a much shorter duration of exposure to high oxygen is sufficient to affect metabolic function. Here we look at the acute effects of MLE-12 cells exposed to 4 h of hyperoxia (95% O₂, 5% CO₂) and at effects sustained with a 24-h recovery in air (21% O₂, 5% CO₂). We found that a short exposure caused dysregulation of glucose utilization and reduced oxphos and ATP production. With a 24-h recovery, cells sustained metabolic dysregulation and reduced mitochondrial fuel utilization. Furthermore, 4 h of hyperoxia was sufficient to induce changes in mitochondrial dynamics, although these changes recovered after 24 h. Additionally, neonatal mice exposed to hyperoxia for as little as 12 h show lasting alveolar simplification at postnatal day 14 (PND 14).

METHODS

Cell lines, culture, and hyperoxia

MLE-12 cells were purchased from ATCC. Cells were cultured in Dulbecco's Modified Eagle Medium/F12 media containing 2% fetal bovine serum, insulin (5 µg/mL), transferrin (10 µg/mL), sodium selenite (30 nM), hydrocortisone (10 nM), β-estradiol (10 nM), HEPES (10 nM), and glutamine (2 mM). In air, cells were maintained at 37 °C (21% O₂, 5% CO₂). In the acute model, cells were exposed to 4 h of hyperoxia (95% O₂, 5% CO₂). In the recovery model, cells were exposed to 4 h of hyperoxia (95% O₂, 5% CO₂) and then placed in air (21% O₂, 5% CO₂) for 24 h.

Mouse hyperoxic exposure and lung morphology

Newborn C57BL/6J mice (<12 h old) along with their mothers were exposed to room air or hyperoxia (>95% O₂) for 12 or 24 h in an A-chamber (BioSpherix, Redfield, NY).¹⁵ Pups were allowed to recover in room air until time of harvest. Radial alveolar count (RAC) was measured as described.¹⁶ In brief, lungs were perfused with phosphate-buffered saline (PBS), inflated with 1% low melt agarose in PBS using 100 µL/g body weight, fixed with 4% paraformaldehyde, and embedded in paraffin. Lungs were sectioned into 5-µm sections and stained with hematoxylin and eosin (H&E). A perpendicular line was drawn from the center of a respiratory bronchiole to the nearest connective tissue septum and the number of alveoli intersected by this line was counted as RAC. All animal experiments were reviewed and approved by the Institutional Animal Care and Use Committee of Brown University.

Mitochondrial stress test

Oxphos was measured using the XF^o24 Seahorse Bioanalyzer (Agilent) following the manufacturer's instructions. In the acute model, cells were seeded in seahorse assay plates 24 h in air (21% O₂/5% CO₂) prior to assay. The day of the assay, cells were exposed to hyperoxia for 4 h. In the recovery model, cells were exposed to 4 h of hyperoxia, trypsinized, counted, and seeded in Seahorse plates in air for 24 h. Immediately prior to the assay, cells were confirmed to be evenly seeded and one well from each condition was counted by trypan blue exclusion and used for normalization.

Evaluation of electron flow

Cells were plated and normalized as above and the XF^o24 Seahorse Bioanalyzer was used to measure oxygen consumption rate (OCR). Activity was assessed in 1× MAS buffer (described in XF Plasma Membrane Permeabilizer Guide (PMP); Agilent) including 10 mM pyruvic acid, 2 mM malate, 4 µM FCCP, 4 mM ADP, 0.2% (w/v) fatty acid-free bovine serum albumin, and 1 nM PMP reagent. Final concentrations of the injected reagents were: 2 µM rotenone,

10 mM succinate, 1.5 µg/mL antimycin A, 10 mM ascorbate, and 100 µM tetramethyl-*p*-phenylenediamine (TMPD).

Metabolic pathway analysis

Cells were harvested after exposures and resuspended in 1× MAS buffer. Cells were filtered through a 70-micron nylon filter (cell strainer, Falcon 352350) to remove clumps. Cells were counted to determine their viability with trypan blue. The cells had viability >95%. According to manufacturer's instructions (Biolog), 30 µL per well of the Assay Mix were pipetted into all wells and incubated at 37 °C for 1 h to allow substrates to fully dissolve, followed by addition of 30 µL cell suspension to all wells. The MitoPlate was read for 4 h at OD590 on a microplate reader in kinetic mode.

Iron measurement

Non-heme iron concentrations were quantified using inductively coupled plasma optical emission spectroscopy (Model Optima 4300D, Perkin Elmer, Norwalk, CT) operated at wavelengths of 238.204 and 259.939 nm.

Determination of steady-state mRNA levels

Total RNA was isolated by using the RNeasy Kit (Qiagen). Reverse transcription was performed with MultiScribe reverse transcriptase (Invitrogen). Taqman Universal PCR Master Mix and Taqman probes were from ThermoFisher: Opa1 (Mm01349707), Mfn1 (Mm00612599), Mfn2 (Mm00500120), Dnm1 (Mm01342903), Drp1 (Mm01342903), MTP18 (Mm00466042), Fis1 (Mm00481580), PPARγ (Mm01184322), PGC1α (Mm01208835), TFAM (Mm00447485), TIM23 (Mm03010822), and HO-1 (Mm00516006)

Determination of protein levels and activity

Western blotting was used to measure the relative protein levels as previously described.¹⁷ Briefly, protein lysates were run on a 4–12% sodium dodecyl sulfate polyacrylamide gel (Invitrogen) and transferred to a polyvinylidene difluoride membrane, which were incubated with the following primary antibodies: TOM20 (Cell Signaling 42406s), transferrin receptor (ThermoFisher 13-6800), ferritin (ab75973), and 5,5-dimethyl-1-pyrroline *N*-oxide (DMPO; a kind gift of Ron Mason). Appropriate horseradish peroxidase-conjugated secondary antibodies were used for visualization with Luminata Crescendo (EMD Millipore) or Super-Signal West Femto substrate (ThermoFisher) using the ChemiDoc Touch Imaging System (BioRAD). The in-gel aconitase activity was conducted as described.¹⁸

Proliferation assays

To examine proliferation, cells were labeled with 5-ethynyl-2'-deoxyuridine (EdU) Alexa Fluor 488 (C10425, ThermoFisher) according to the instructions. For viability, cells were labeled with propidium iodide (P1304MP, ThermoFisher) according to the instructions. Fluorescence intensity was measured using a BD FACSAria flow cytometer and analyzed with FlowJo V10. We seeded 400,000 MLE-12 cells/well in a 6-well plate in triplicate.

Super-resolution imaging of mitochondria

Cells were visualized utilizing Cytiva DeltaVision OMX SR super-resolution microscope system (Cytiva). Structured illumination is an imaging technique that generates super-resolved images through the interaction of structured light patterns with sample. Computer algorithms process the collected raw data set and generate the final super-resolution image.

Fluorescent labeling of mitochondria

Cells were labeled with Mitotracker Green FM (M7514, ThermoFisher), Mitotracker RedCMXRos (M7512m ThermoFisher), and tetramethylrhodamine methyl ester (TMRM; T668, ThermoFisher) according to the instructions. Fluorescence intensity was

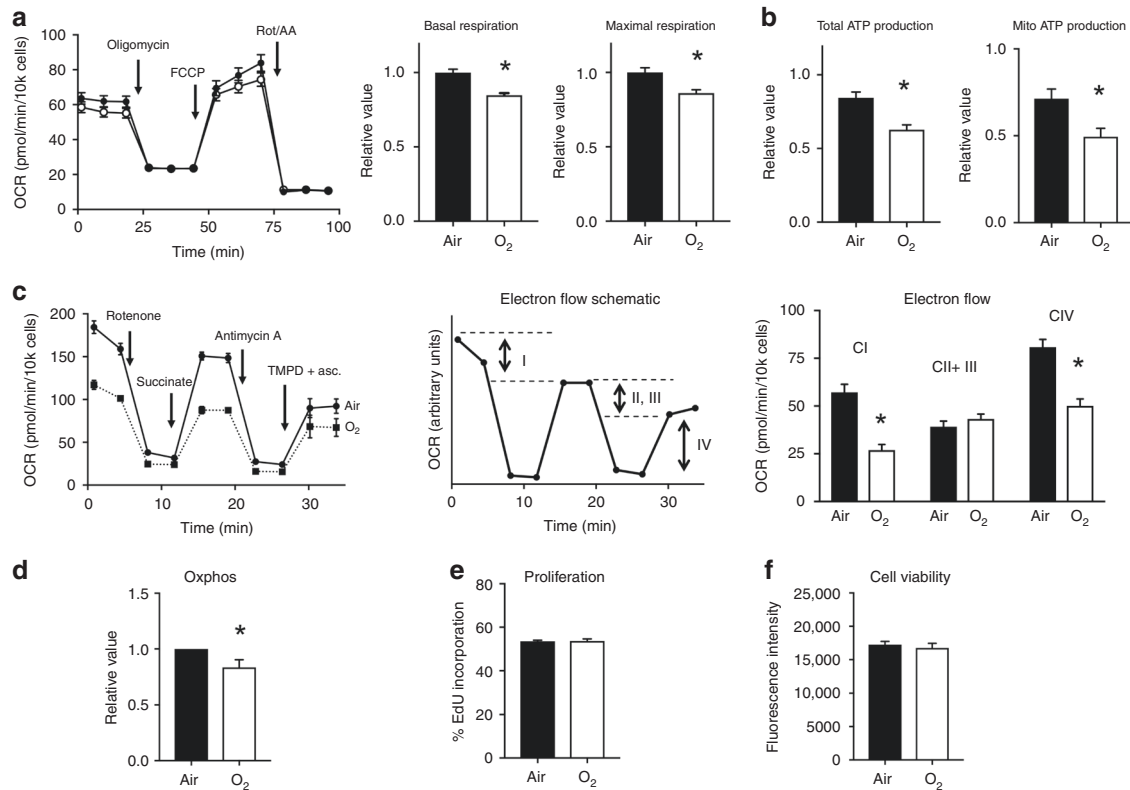


Fig. 1 Four hours of hyperoxia is sufficient to cause dysregulation of oxphos, ETC, and energy production. **a** Oxygen consumption rate (OCR) was measured with the Seahorse mitochondrial stress test; a representative trace is shown. Basal and maximal respiration was determined according to the manufacturer's instructions. **b** Production of total and mitochondrial ATP were measured with the Seahorse ATP rate assay. **c** Activity of electron transport chain complexes was determined by a Seahorse electron flow assay. **d** Oxidative phosphorylation was determined via the Biolog MitoPlate. **e** Cell proliferation was measured by EdU incorporation and FACS analysis. **f** Cell viability measured by propidium iodide inclusion/exclusion and FACS analysis. Closed bars represent air-exposed cells, and open bars represent cells exposed to hyperoxia for 4 h. * $p < 0.05$ vs air.

measured using a BD FACSria flow cytometer and analyzed with FlowJo V10.

Statistical analysis

All experiments with MLE-12 cells had a minimum of three biological replicates. Error bars are reported as the mean \pm standard error of the mean (SEM) for all values. Graph Pad Prism 6 software was used to do unpaired Student's *t* tests for comparisons between two groups, with a $p < 0.05$ used as a threshold for significance.

RESULTS

Four hours of hyperoxia reduces oxphos in MLE-12 cells

In mouse lung epithelial cells, it was previously shown that 24 h of hyperoxia reduced oxphos¹⁴ but we wished to know whether a shorter exposure would alter metabolism. We used a mitochondrial stress test to measure OCR in a Seahorse Bioanalyzer and found a reduction in basal respiration and maximum respiration after 4 h of hyperoxia compared to air (Fig. 1a). Cells exposed to 8 h of hyperoxia had a further reduction in basal and maximal respiration, demonstrating a dose-dependency (Supplementary Fig. 1). The reduction in oxphos at 4 h was associated with dysregulated energy production, as the Seahorse ATP production assay showed a reduction in the total amount of ATP generated and ATP produced by mitochondria (Fig. 1b). We next utilized a glycolytic rate assay, which measures the glycolytic proton efflux rate, to examine glycolysis. We found no changes in basal glycolysis or the glycolytic response to inhibition of oxphos,

termed compensatory glycolysis, indicating that 4 h of hyperoxia does not alter glycolysis (data not shown).

We wondered whether the reduced oxphos observed with 4 h of hyperoxia changes the activity of complexes in the electron transport chain (ETC). Using permeabilized cells, we interrogated various ETC complexes as illustrated schematically (Fig. 1c). The flow of electrons from complex I through IV is halted at CI by administration of rotenone, followed by the regeneration of electron flow at CII with injection of succinate. Electron flow is stopped at CIII by antimycin A but is then resumed by administration of TMPD/ascorbate to determine function of complex IV. We found that cells exposed to 4 h of hyperoxia exhibited reduced electron flow at complexes I and IV (Fig. 1c).

We also used a different assay to assess mitochondrial function, the Biolog MitoPlate. This assay can measure oxidation of individual substrates and ETC function with a colorimetric assay. We show that, in the absence of any exogenous substrates, the utilization of endogenous substrates was reduced significantly in cells exposed to hyperoxia (Fig. 1d). Since mitochondrial function is vital in maintaining global cellular processes, we also examined cell proliferation and viability. However, we found no change in proliferation, measured by EdU incorporation, and no change in viability, measured by propidium iodide incorporation/exclusion, with 4 h hyperoxia (Fig. 1e, f).

Some metabolic defects persist with 24 h of recovery

To determine whether the effects observed at 4 h persisted, we exposed MLE-12 cells to hyperoxia and allowed them to recover in air for 24 h and examined metabolism. Glycolysis was still

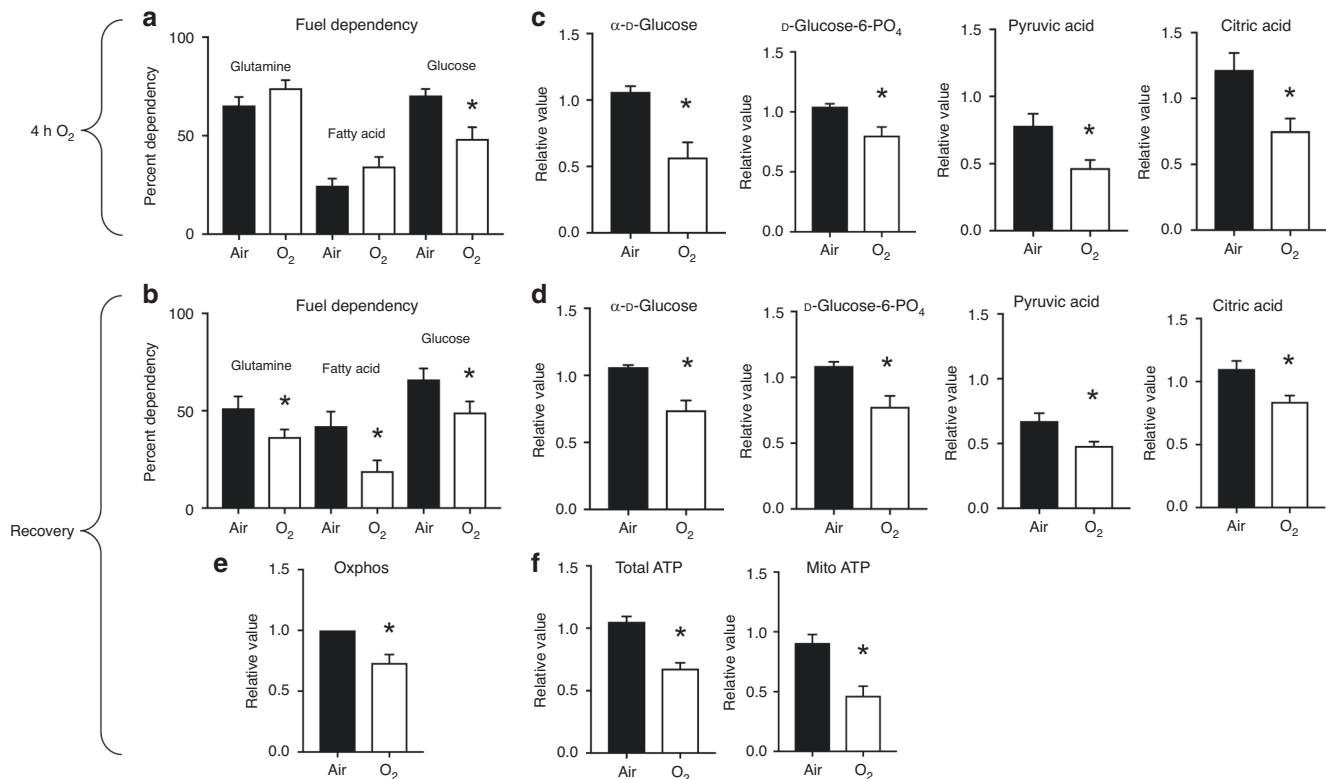


Fig. 2 Four hours of hyperoxia causes a persistent reduction in fuel utilization. **a, b** Dependencies for glutamine, fatty acid, and glucose were measured by the Seahorse fuel utilization assay. **c, d** Utilization of glycolytic and tricarboxylic acid (TCA) cycle metabolites were determined by the Biolog MitoPlate. **e** Oxidative phosphorylation with 24 h recovery was determined via Biolog MitoPlate. **f** Production of total and mitochondrial ATP with 24 h recovery was measured with the Seahorse ATP rate assay. Cells were grown in air (closed bars) or 4 h of hyperoxia (open bars) (**a, c**) followed by 24 h air recovery (**b–f**). * $p < 0.05$ vs air.

unchanged in recovery (data not shown). In the mitochondrial stress test, OCR returned to baseline, as indicated by no change in basal respiration or maximum respiration (Supplementary Fig. 2A). Equally, changes in electron flow seen acutely at 4 h were now restored with 24 h of air recovery, and there was still no effect on cell proliferation or viability (Supplementary Fig. 2B–D).

In order to expand our understanding of the observed metabolic defects, we conducted two distinct assays to better understand mitochondrial fuel utilization, both acutely and with air recovery. The Seahorse fuel utilization assay examines glucose, glutamine, and fatty acid consumption; we found that cells exposed to 4 h hyperoxia had reduced utilization of glucose only (Fig. 2a) but that in recovery cells had reduced utilization of all three fuels (Fig. 2b). Using the Biolog MitoPlate, we also saw acute reduction of glucose (α -D-glucose) utilization and reduction in use of downstream glycolytic intermediates D-glucose-6-PO₄ and pyruvic acid, as well as tricarboxylic acid (TCA) substrate citric acid (Fig. 2c). Reduction in utilization of these substrates persisted with 24 h air recovery (Fig. 2d). In addition, specifically in recovery, we saw reduced utilization of TCA cycle intermediates *cis*-aconitic acid, isocitric acid, α -keto-glutaric acid and amino acids, including glutamine, and ketone bodies (Supplementary Fig. 3). Additionally the mitochondrial utilization of endogenous substrates assessed with the Biolog plate remained reduced (Fig. 2e) as did the amount of total ATP production and ATP from mitochondria (Fig. 2f).

Short hyperoxic exposure is not sufficient to induce widespread oxidative damage
High levels of oxygen have been shown to cause damage to macromolecules and to dysregulate cellular processes, including metabolism.^{19–21} Previous studies have focused on the role of

oxidative stress in the deleterious effects of hyperoxia on mitochondria.^{22–25} Thus we wished to examine various markers of oxidative stress after 4 h hyperoxia and in recovery. We examined superoxide production in live cells with MitoSOX Red staining and fluorescence-activated cell sorter (FACS) analysis and saw no difference at 4 h (Fig. 3a). We looked at protein nitron adducts using a DMPO spin trap antibody and saw no differences acutely or in recovery (Fig. 3a). Equally we saw no changes in the expression of the antioxidant response protein HO-1 or mitochondrial superoxide dismutase (Fig. 3a).

Our substrate utilization results indicated a reduction in mitochondrial utilization of citric acid, which is catalyzed by mitochondrial aconitase. Aconitases can serve as oxygen sensors, as their activities depend on iron-sulfur clusters, which are particularly sensitive to disruption by oxygen.²⁶ Using an in-gel aconitase assay, which distinguishes cytosolic from mitochondrial aconitase, we saw no change at 4 h hyperoxia in mitochondrial aconitase activity but did see reduction of cytosolic aconitase (Fig. 3b). Cytosolic aconitase activity returned to baseline in recovery (data not shown). To explore the potential role of disrupted iron homeostasis after 4 h exposure, we examined levels of the iron storage protein ferritin and found that it was reduced, while the levels of iron importer transferrin receptor were unchanged (Supplementary Fig. 4A, B). This raised the possibility that iron might be limiting so we measured total cellular non-heme iron but found no difference between air and 4 h hyperoxia (Supplementary Fig. 4C).

In order to evaluate mitochondrial membrane potential, we stained cells with TMRM and found no reduction in fluorescence by FACS either after 4 h hyperoxia or in recovery (Supplementary Fig. 5A). As measured by Seahorse OCR in the mitochondrial stress test, we also do not see any changes in proton leak indicating that

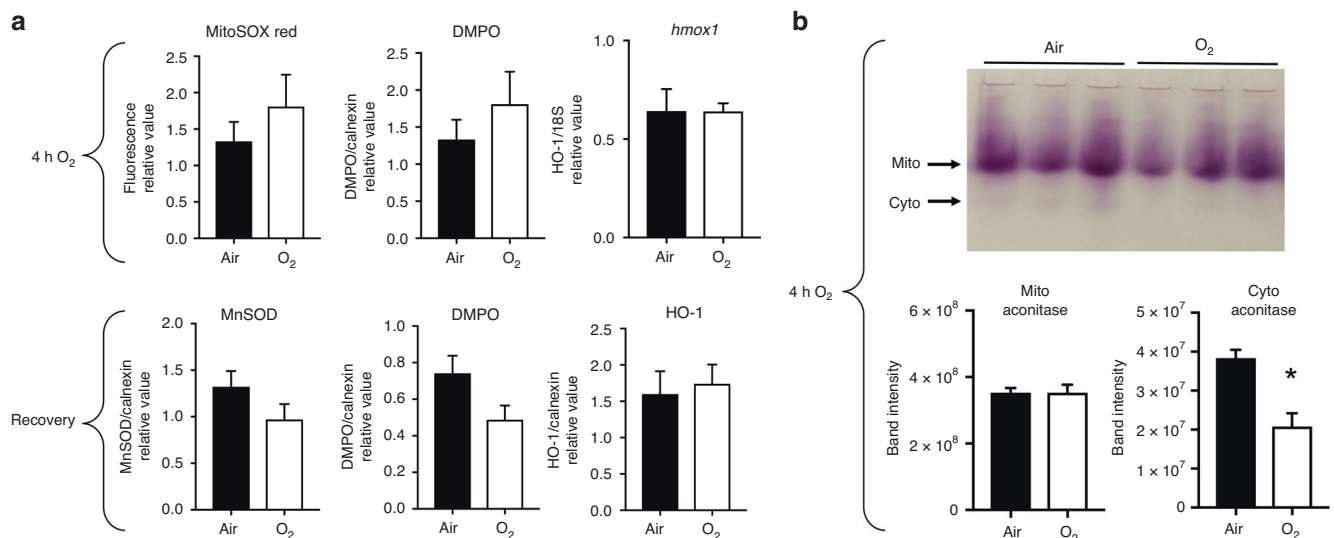


Fig. 3 Four hours of hyperoxia does not cause oxidative stress or depolarization of mitochondria. **a** Oxidative stress at 4 h hyperoxia was determined by measuring the fluorescence signal of MitoSox Red using FACS, 5,5-dimethyl-1-pyrroline *N*-oxide (DMPO) reactive oxygen species adducts by western blot, and heme oxygenase 1 (*hmx1*) by Taqman. Oxidative stress with 24 h recovery was examined by western blot for manganese superoxide dismutase (MnSOD), DMPO, and HO-1. **b** Aconitase activity at 4 h of hyperoxia was measured utilizing an in-gel aconitase assay, loading 65 μg lysate per lane. Closed bars represent air-exposed cells, and open bars represent cells exposed to hyperoxia for 4 h acutely or with 24 h recovery, as indicated. **p* < 0.05 vs air.

mitochondria are not depolarized (Supplementary Fig. 5B). We wanted to determine whether there was decreased mitochondrial biogenesis, which could explain the observed reduction in oxphos. We found that the expression levels of mitochondrial biogenesis transcription factors, TFAM, PGC1α, and PPARγ, all remained unchanged after 4 h of hyperoxia and in recovery (Supplementary Fig. 6A). We also examined the levels of mitochondrial membrane proteins TIMM23 and TOMM20 acutely and in recovery as a proxy for the number of mitochondria, and these remained unchanged (Supplementary Fig. 6B)

Short hyperoxic exposure alters mitochondrial morphology

Others have demonstrated that a 6-h hyperoxic exposure is sufficient to cause mitochondrial fragmentation.²⁷ We wanted to determine whether our shorter exposure to hyperoxia would similarly dysregulate mitochondrial dynamics. We found an increase in mRNA levels of fusion proteins *Mfn1* and *Opa1* acutely but these returned to baseline in recovery (Fig. 4a). No changes in the gene expression of fission proteins *Drp1*, *Fis1*, or *Mtp18* were observed acutely, but we saw decreased expression of these proteins in recovery, possibly indicating a protective response in recovery (Fig. 4b). To address whether hyperoxia induces mitochondrial mass changes, we utilized MitoTracker Green stain and measured fluorescent signal by FACS. We observed increased fluorescence suggesting an increase in mitochondrial mass of cells exposed to 4 h of hyperoxia, which then returned to baseline in recovery (Fig. 4c).

Next we performed structured illumination microscopy (SIM) to examine mitochondrial morphology with MitoTracker Red CMXRos. In air controls, mitochondria appeared as discrete spheroid organelles that are distributed densely in the perinuclear area (Fig. 5a–d). Upon exposure to 4 h of hyperoxia, the cells demonstrated significant changes in mitochondrial morphology and distribution fitting the transcriptional changes in fusion genes. The mitochondria appeared more evenly distributed across the whole cytoplasmic surface and formed highly elongated and interconnected tubular networks, indicative of a fusion process (Fig. 5e–h). Finally, mitochondria returned to control-level morphology and distribution with perinuclear clustering of discrete mitochondria after 24 h of air recovery (Fig. 5i–l). The

increased fusion seen by SIM with 4 h hyperoxia correlates with the increased mitochondrial mass measurement using FACS (Fig. 4c). Increased mitochondrial mass is likely reflective of the mass of “clusters” of fused mitochondria.

Neonatal mice exposed to hyperoxia for 12 h exhibit alveolar simplification

We show that MLE-12 cells exposed to 4 h of hyperoxia have metabolic defects that persist with a 24-h air recovery (Fig. 2). We wished to know whether the detrimental effects of a short hyperoxic exposure in a single lung cell type would extend to a more physiological model of neonatal chronic lung disease. Thus we exposed neonatal mice to air or hyperoxia for 12 or 24 h followed by recovery in air until PND 14. As seen by H&E staining, as few as 12 h of hyperoxia caused alveolar simplification and increased airspaces (Fig. 6a). RAC were performed to quantify diminished alveolar complexity and indicated that mice exposed to 12 h of hyperoxia were significantly compromised compared to air controls (Fig. 6b). Twenty-four hours of hyperoxia reduced alveolar complexity even further, indicating a dose-dependent response (Fig. 6b). Interestingly, we observed resolution of alveolar damage at PND 60 following a 24-h neonatal hyperoxia exposure (data not shown). Whether a second insult would lead to increased susceptibility to injury is yet to be determined.

DISCUSSION

In this study, MLE-12 cells were used to examine the effects of 4 h of hyperoxia (95% O₂, 5% CO₂) on mitochondrial function. We found that this very short exposure to hyperoxia dysregulated glucose utilization by mitochondria and reduced oxphos and ATP production. Cells allowed to recover in air for 24 h show sustained metabolic dysregulation and reduced fuel utilization. With 4 h of hyperoxia, we also observed changes in mitochondrial dynamics, but this did not persist in recovery. Additionally, we found that as little as 12 h of exposure of neonatal mice to hyperoxia is sufficient to cause lasting alveolar simplification, which is clinically relevant as there are cases where neonates are briefly exposed to hyperoxia as life-saving measures.

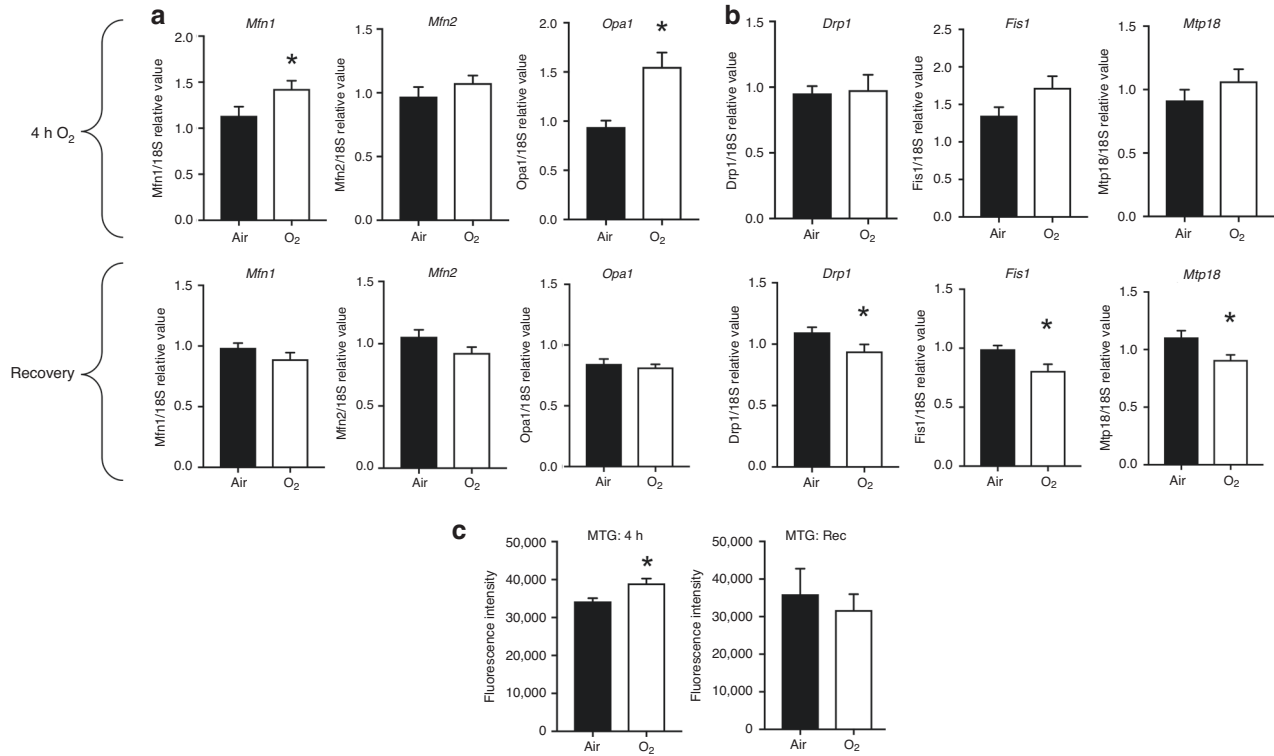


Fig. 4 Four hours of hyperoxia causes an increase in expression of fusion proteins and mitochondrial mass, which does not persist in recovery. **a** Gene expression of fusion proteins (*Mfn1*, *Mfn2*, *Opa1*) measured by Taqman acutely (top) and with 24 h recovery (bottom). **b** Gene expression of fission proteins (*Drp1*, *Fis1*, *Mtp18*) measured by Taqman acutely (top) and with 24 h recovery (bottom). **c** Mitochondrial mass was determined by measuring the fluorescence signal of MitoTracker Green (MTG) using FACS at 4 h and with 24 h recovery (rec). Closed bars represent air-exposed cells and open bars represent cells exposed to hyperoxia for 4 h acutely or with 24 h recovery as indicated. * $p < 0.05$ vs air.

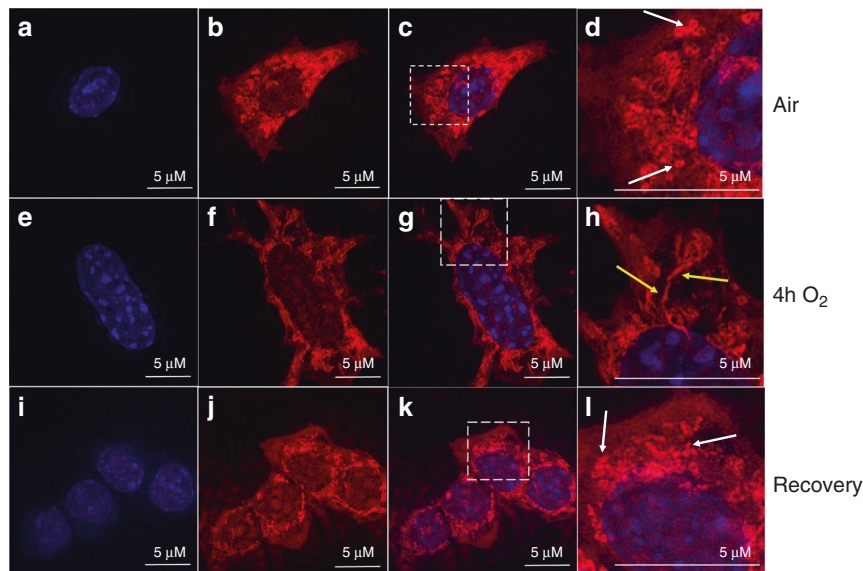


Fig. 5 Four hours of hyperoxia causes mitochondria to form elongated interconnected networks, which does not persist in recovery. **a–d** Images of air control cells stained with 4',6-diamidino-2-phenylindole (DAPI) (**a**) and MitoTracker Red CMXRos (**b**). **c** Merged image and **d** magnified image of dotted box in **c**. **d** White arrows show round mitochondrial morphology. **e–h** Images of cells exposed to 4 h hyperoxia and displayed as **a–d**. **h** Yellow arrows show elongated interconnected mitochondrial networks. **i–l** Images of cells exposed to 4 h of hyperoxia followed by 24 h recovery and displayed as **a–d**. **l** White arrows show round mitochondrial morphology.

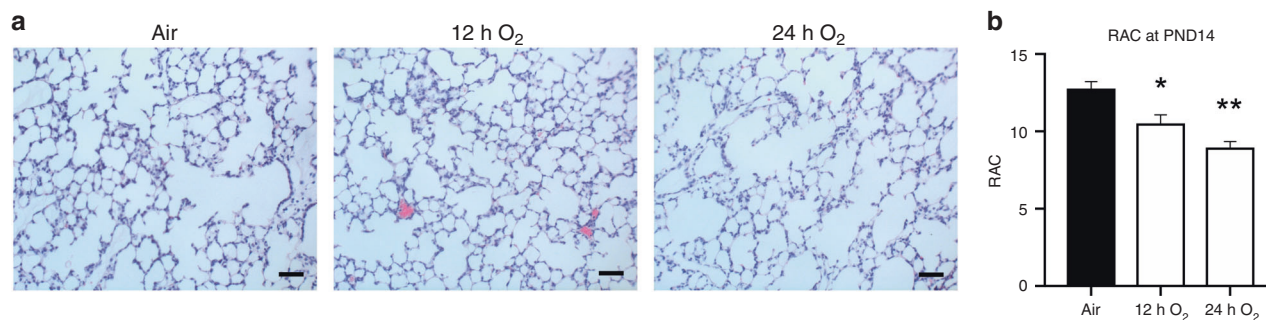


Fig. 6 Neonatal short-term hyperoxic exposure impairs mouse lung growth. C57BL/6J neonatal mice (<12 h old) were exposed to air or hyperoxia (95% O₂) for 12 or 24 h. Mice were allowed to recover in room air until PND 14. **a** Representative images of lung tissues stained with H&E. Bar size: 100 μm. **b** Radial alveolar counts (RAC) were assessed in mouse lungs after mice were exposed to air or hyperoxia for 12 or 24 h as neonates. N = 5–7. **p* < 0.05 vs air; ***p* < 0.05 vs 12 h O₂.

A prior study demonstrated that exposure of MLE-12 cells to hyperoxia for 24 h did not alter basal glycolysis, and we too observe no changes at 4 h.¹⁴ That study also demonstrated reduced activity of overall oxphos and of ETC complexes I and II. Here, with 4 h hyperoxia, we also see reduction of oxphos and reduced activities of complexes I and IV. We cannot be sure what accounts for our differences in complex activities, but it may be due to duration of exposure. A study using A549 cells exposed to hyperoxia for 24 h found an increased rate of glucose consumption approximately twofold to fourfold relative to the air-exposed cells.²⁷ Here we found reduced utilization of glucose and glycolytic metabolites with a 4-h exposure. Even though MLE-12 cells are immortalized, the differences in our findings may be cell-type specific as carcinoma cells like A549 cells are known to display the Warburg effect, in which glycolysis is used as the main source of energy.²⁸

Our observation that oxphos is reduced at 4 h is due to the combined activities of ETC complexes and mitochondrial glucose utilization. In recovery, we observed that glucose utilization remains reduced and that utilization of glutamine and fatty acids was also significantly reduced, demonstrating persistent dysregulation of the TCA cycle. Previous work in our laboratory indicates that lung endothelial cells exposed to hyperoxia with a 24-h recovery displayed increased utilization of fatty acids, highlighting possible cell-specific effects of hyperoxia on metabolism.¹⁵ The observed reduction in oxphos may also be due in part to defects in TCA cycle enzymes. For example, MLE-12 cells exposed to 24 h of hyperoxia exhibited reduced activity of several enzymes, including α-ketoglutarate dehydrogenase and succinate dehydrogenase.¹⁴ In our study, 4 h of hyperoxia did not affect the in vitro activity of mitochondrial aconitase despite the reduced mitochondrial utilization of citric acid in permeabilized cells. The Biolog MitoPlate assay reflects the combined action of substrate utilization and ETC function, thus if ETC activity is reduced as we observed, then substrate utilization may be reduced as well (Fig. 1d). However, in recovery, as electron flow and oxphos measured by the Seahorse are restored, we saw persistent reduction in oxphos measured by the MitoPlate (Fig. 2e). This suggests that ETC function recovers before restoration of mitochondrial fuel utilization. Notably, we did not extend recovery time for cells beyond 24 h, thus we are limited in understanding how persistent these metabolic changes may be.

After 4 h of hyperoxia, we saw reduced in vitro activity of cytosolic aconitase only. Studies have shown that hydrogen peroxide and superoxide cause dysregulation of cytosolic aconitase activity.^{26,29} Other studies using primate and rat lungs showed that mitochondrial aconitase activity was reduced by hyperoxia, but no changes were observed for cytosolic aconitase.^{30,31} Similarly, A549 cells displayed a reduction in mitochondrial aconitase in as short as 3 h of hyperoxia.³⁰ Our data support the view that aconitases are quite sensitive to oxygen; it appears that

cytosolic aconitase activity in MLE-12 cells is disrupted quickly, while the mitochondrial aconitase may be more protected. Since aconitase activity depends on the presence of oxygen-sensitive iron–sulfur clusters, we examined whether iron homeostasis was disrupted with 4 h hyperoxia. Although we found decreased levels of ferritin, we found no difference in the levels of total cellular iron. This does not preclude potential intracellular redistribution of iron, which may warrant further investigation.

The formation of mitochondrial networks that are elongated is promoted by increased fusion or reduced fission, whereas fragmentation is caused by increased fission or reduced fusion. It has been shown that 24 h of hyperoxia causes mitochondrial fragmentation in pulmonary endothelial cells.²⁷ With our short exposure, we observed an increase in transcription of outer and inner membrane fusion proteins *Mfn1* and *Opa1*, which was accompanied by increased mitochondrial mass, although protein levels did not change (data not shown). We also found less mRNA for fission markers *Drp1*, *Fis1*, and *Mtp18* in recovery. Although we do not fully understand these observations, it is possible that posttranslational modifications are involved in regulating fusion and fission activities, as has been shown for *Drp1*.³² Mitochondrial metabolism is tied to mitochondrial dynamics, and it has been shown that fusion is a protective response to metabolic dysregulation.³³ For example, in fibroblasts and B cells, limited metabolite/nutrient availability results in connected elongated mitochondria.^{34,35} Here we see that mitochondria are undergoing a temporary fusion process, creating a hyperelongated tubular network of mitochondria. This morphological change is similar to that seen previously in MLE-12 cells exposed to cigarette smoke extract.³⁶ This indicates that mitochondrial fusion in MLE-12 cells may represent a general morphological change in response to metabolic or environmental stress. However, in that study mitochondrial fusion was associated with an increased metabolic rate,³⁷ whereas in our model the mitochondrial fusion is found alongside a general reduction in cellular metabolism.

In human microvascular endothelial cells, it has been shown that 24 h of hyperoxia causes a reduction in cell proliferation and viability.³⁸ With our short exposure of MLE-12 cells, we do not see changes in proliferation or cell viability. It appears this time point is too early to detect these changes in cell culture, but whether or not 4 h of hyperoxia might lead to increased susceptibility to a second insult may be worth considering. Additionally, it is likely that short neonatal hyperoxic exposure reduces lung cell proliferation and/or viability, as we observed significant loss of alveolar complexity in mice exposed to 12 h of hyperoxia, which was exacerbated with 24 h of exposure. As alveolar simplification was resolved by PND 60, one limitation of our study is that we do not have a detailed picture of the timeline of recovery nor of injury to specific cell types. Equally, the extent of injury is expected to be dose dependent, such that concentrations of oxygen less than the

95% used here would be less deleterious and may resolve on a shorter timeline. Another limitation of this study is that we do not know if the observed lung morphological changes are associated with lung metabolic alterations. It would be of interest to examine ATP production and mitochondrial fuel utilization in the lung, especially since understanding this may present the opportunity to attenuate lung injury with nutritional or metabolic interventions.

ACKNOWLEDGEMENTS

We are grateful to Dr. Ronald Mason for the generous gift of DMPO antibody. Research reported in this publication was supported by the National Heart, Lung, and Blood Institute (NHLBI) of the National Institutes of Health under award number HL139080 (to D.G.), NIH T32 HL134625 (to D.G.), the Institutional Development Award (IDeA) from the NIGMS of NIH under grant #P20GM103652 (to H.Y.), the Falk Medical Research Trust Catalyst Award (to H.Y.), and the Warren Alpert Foundation at Brown University (to P.A.D.).

AUTHOR CONTRIBUTIONS

Conception and design: D.G., P.A.D. Acquisition and analysis of data: all authors. Drafting and revising the paper and final approval of the version to be published: D.G., J.F.C., P.A.D.

ADDITIONAL INFORMATION

The online version of this article (<https://doi.org/10.1038/s41390-020-01224-5>) contains supplementary material, which is available to authorized users.

Competing interests: The authors declare no competing interests.

Patient consent: Patient consent was not required for this study.

Publisher's note Springer Nature remains neutral with regard to jurisdictional claims in published maps and institutional affiliations.

REFERENCES

- Nardiello, C. et al. Standardisation of oxygen exposure in the development of mouse models for bronchopulmonary dysplasia. *Dis. Model Mech.* **10**, 185–196 (2017).
- Saugstad, O. D. Is oxygen more toxic than currently believed? *Pediatrics* **108**, 1203–1205 (2001).
- Vento, M. et al. Preterm resuscitation with low oxygen causes less oxidative stress, inflammation, and chronic lung disease. *Pediatrics* **124**, e439–e449 (2009).
- Khaw, K. S. & Ngan Kee, W. D. Fetal effects of maternal supplementary oxygen during caesarean section. *Curr. Opin. Anaesthesiol.* **17**, 309–313 (2004).
- White, L. N. et al. Achievement of saturation targets in preterm infants <32 weeks' gestational age in the delivery room. *Arch. Dis. Child. Fetal Neonatal Ed.* **102**, F423–F427 (2017).
- Wang, Y. et al. Pulmonary alveolar type I cell population consists of two distinct subtypes that differ in cell fate. *Proc. Natl Acad. Sci. USA* **115**, 2407 (2018).
- Ray, N. B. et al. Dynamic regulation of cardiolipin by the lipid pump Atp8b1 determines the severity of lung injury in experimental pneumonia. *Nat. Med.* **16**, 1120–1127 (2010).
- Budinger, G. R. et al. Epithelial cell death is an important contributor to oxidant-mediated acute lung injury. *Am. J. Respir. Crit. Care Med.* **183**, 1043–1054 (2011).
- Nabhan, A. N., Brownfield, D. G., Harbury, P. B., Krasnow, M. A. & Desai, T. J. Single-cell Wnt signaling niches maintain stemness of alveolar type 2 cells. *Science* **359**, 1118–1123 (2018).
- Mishra, P. & Chan, D. C. Mitochondrial dynamics and inheritance during cell division, development and disease. *Nat. Rev. Mol. Cell Biol.* **15**, 634–646 (2014).
- Mishra, P., Carelli, V., Manfredi, G. & Chan, David C. Proteolytic cleavage of Opa1 stimulates mitochondrial inner membrane fusion and couples fusion to oxidative phosphorylation. *Cell Metab.* **19**, 630–641 (2014).
- Mizumura, K. et al. Mitophagy-dependent necroptosis contributes to the pathogenesis of COPD. *J. Clin. Investig.* **124**, 3987–4003 (2014).
- Lottes, R. G., Newton, D. A., Spyropoulos, D. D. & Baatz, J. E. Alveolar type II cells maintain bioenergetic homeostasis in hypoxia through metabolic and molecular adaptation. *Am. J. Physiol. Lung Cell Mol. Physiol.* **306**, L947–L955 (2014).
- Das, K. C. Hyperoxia decreases glycolytic capacity, glycolytic reserve and oxidative phosphorylation in MLE-12 cells and inhibits complex I and II function, but not complex IV in isolated mouse lung mitochondria. *PLoS ONE* **8**, e73358 (2013).
- Yao, H. et al. Fatty acid oxidation protects against hyperoxia-induced endothelial cell apoptosis and lung injury in neonatal mice. *Am. J. Respir. Cell Mol. Biol.* **60**, 667–677 (2019).
- Cooney, T. P. & Thurlbeck, W. M. The radial alveolar count method of Emery and Mithal: a reappraisal 1-postnatal lung growth. *Thorax* **37**, 572–579 (1982).
- Towbin, H., Staehelin, T. & Gordon, J. Electrophoretic transfer of proteins from polyacrylamide gels to nitrocellulose sheets: procedure and some applications. *Proc. Natl Acad. Sci. USA* **76**, 4350–4354 (1979).
- Tong, W. H. & Rouault, T. A. Functions of mitochondrial ISCU and cytosolic ISCU in mammalian iron-sulfur cluster biogenesis and iron homeostasis. *Cell Metab.* **3**, 199–210 (2006).
- McGrath-Morrow, S. A., Cho, C., Soutiere, S., Mitzner, W. & Tuder, R. The effect of neonatal hyperoxia on the lung of p21Waf1/Cip1/Sdi1-deficient mice. *Am. J. Respir. Cell Mol. Biol.* **30**, 635–640 (2004).
- McGrath-Morrow, S. A. & Stahl, J. Apoptosis in neonatal murine lung exposed to hyperoxia. *Am. J. Respir. Cell Mol. Biol.* **25**, 150–155 (2001).
- O'Reilly, M. & Thebaud, B. Animal models of bronchopulmonary dysplasia. The term rat models. *Am. J. Physiol. Lung Cell. Mol. Physiol.* **307**, L948–L958 (2014).
- Farrow, K. N. et al. Brief hyperoxia increases mitochondrial oxidation and increases phosphodiesterase 5 activity in fetal pulmonary artery smooth muscle cells. *Antioxid. Redox Signal.* **17**, 460–470 (2012).
- Farrow, K. N. et al. Mitochondrial oxidant stress increases PDE5 activity in persistent pulmonary hypertension of the newborn. *Respir. Physiol. Neurobiol.* **174**, 272–281 (2010).
- Ratner, V., Sosunov, S. A., Niatsetskaia, Z. V., Utkina-Sosunova, I. V. & Ten, V. S. Mechanical ventilation causes pulmonary mitochondrial dysfunction and delayed alveolarization in neonatal mice. *Am. J. Respir. Cell Mol. Biol.* **49**, 943–950 (2013).
- Waxman, A. B. & Kolliputi, N. IL-6 protects against hyperoxia-induced mitochondrial damage via Bcl-2-induced Bak interactions with mitofusins. *Am. J. Respir. Cell Mol. Biol.* **41**, 385–396 (2009).
- Gardner, P. R., Raineri, L., Epstein, L. B. & White, C. W. Superoxide radical and iron modulate aconitase activity in mammalian cells. *J. Biol. Chem.* **270**, 13399–13405 (1995).
- Ma, C. et al. Hyperoxia causes mitochondrial fragmentation in pulmonary endothelial cells by increasing expression of pro-fission proteins. *Arterioscler. Thromb. Vasc. Biol.* **38**, 622–635 (2018).
- Allen, C. B. & White, C. W. Glucose modulates cell death due to normobaric hyperoxia by maintaining cellular ATP. *Am. J. Physiol.* **274**, L159–L164 (1998).
- Pantopoulos, K. & Hentze, M. W. Rapid responses to oxidative stress mediated by iron regulatory protein. *EMBO J.* **14**, 2917–2924 (1995).
- Gardner, P. R., Nguyen, C. D. & White, C. W. Aconitase is a sensitive and critical target of oxygen poisoning in cultured mammalian cells and in rat lungs. *Proc. Natl Acad. Sci. USA* **91**, 12248–12252 (1994).
- Morton, R. L., Iklé, D. & White, C. W. Loss of lung mitochondrial aconitase activity due to hyperoxia in bronchopulmonary dysplasia in primates. *Am. J. Physiol. Lung Cell. Mol. Physiol.* **274**, L127–L133 (1998).
- Wang, Z. W. et al. Mitochondrial fission mediated cigarette smoke-induced pulmonary endothelial injury. *Am. J. Respir. Cell Mol. Biol.* <https://doi.org/10.1165/rcmb.2020-0008OC> (2020).
- Yao, C.-H. et al. Mitochondrial fusion supports increased oxidative phosphorylation during cell proliferation. *Elife* **8**, e41351 (2019).
- Gomes, L. C., Di Benedetto, G. & Scorrano, L. During autophagy mitochondria elongate, are spared from degradation and sustain cell viability. *Nat. Cell Biol.* **13**, 589–598 (2011).
- Molina, A. J. A. et al. Mitochondrial networking protects beta-cells from nutrient-induced apoptosis. *Diabetes* **58**, 2303–2315 (2009).
- Ballweg, K., Mutze, K., Königshoff, M., Eickelberg, O. & Meiners, S. Cigarette smoke extract affects mitochondrial function in alveolar epithelial cells. *Am. J. Physiol. Lung Cell. Mol. Physiol.* **307**, L895–L907 (2014).
- Meiners, S. & Ballweg, K. Proteostasis in pediatric pulmonary pathology. *Mol. Cell. Pediatr.* **1**, 11 (2014).
- Attaye, I. et al. The effects of hyperoxia on microvascular endothelial cell proliferation and production of vaso-active substances. *Intensive Care Med. Exp.* **5**, 22 (2017).